

# Extremely strong spin-orbit coupling effect in light element altermagnetic materials

Shuai Qu<sup>1,3</sup>, Ze-Feng Gao<sup>1,2,3</sup>, Hao Sun<sup>2</sup>, Kai Liu<sup>1,3</sup>, Peng-Jie Guo<sup>1,3,\*</sup> and Zhong-Yi Lu<sup>1,3†</sup>

1. Department of Physics and Beijing Key Laboratory of Opto-electronic Functional Materials & Micro-nano Devices. Renmin University of China, Beijing 100872, China

2. Gaoling School of Artificial Intelligence, Renmin University of China, Beijing, China and

3. Key Laboratory of Quantum State Construction and Manipulation (Ministry of Education), Renmin University of China, Beijing 100872, China

(Dated: January 23, 2024)

Spin-orbit coupling is a key to realize many novel physical effects in condensed matter physics, but the mechanism to achieve strong spin-orbit coupling effect in light element antiferromagnetic compounds has not been explored. In this work, based on symmetry analysis and the first-principles electronic structure calculations, we demonstrate that strong spin-orbit coupling effect can be realized in light element altermagnetic materials, and propose a mechanism for realizing the corresponding effective spin-orbit coupling. This mechanism reveals the cooperative effect of crystal symmetry, electron occupation, electronegativity, electron correlation, and intrinsic spin-orbit coupling. Our work not only promotes the understanding of light element compounds with strong spin-orbit coupling effect, but also provides an alternative for realizing light element compounds with an effective strong spin-orbit coupling.

*Introduction.* Spin-orbit coupling (SOC) is ubiquitous in realistic materials and crucial for many novel physical phenomena emerging in condensed matter physics, including topological physics [1–3], anomalous Hall effect [4], spin Hall effect [5, 6], magnetocrystalline anisotropy [7] and so on. For instance, quantum anomalous Hall (QAH) insulators are characterized by non-zero Chern numbers [8]. The Chern number is derived from the integration of Berry curvature over the occupied state of the Brillouin zone (BZ). For collinear ferromagnetic and antiferromagnetic systems, the integral of Berry curvature over the occupied state of the Brillouin zone must be zero without SOC due to the spin symmetry  $\{C_{\frac{1}{2}}^{\perp}|T\}$ . Here the  $C_{\frac{1}{2}}^{\perp}$  and  $T$  represent the 180 degrees rotation perpendicular to the spin direction and time-reversal operation, respectively. Therefore, QAH effect can only be realized in collinear magnetic systems when SOC is included [9, 10]. On the other hand, strong SOC may open up a large nontrivial bandgap, which is very important to realize QAH effect at high temperatures. In general, strong SOC exists in heavy element compounds. Unfortunately, the chemical bonds of heavy element compounds are weaker than those of light element compounds, which leads to more defects in heavy element compounds. Thus, the stability to realize exotic functionalities in heavy element compounds is relatively weak.

An interesting question is whether the strong SOC effect can be achieved in light element compounds. Very recently, Li et al. demonstrated that the SOC can be enhanced in light element ferromagnetic materials, which derives from the cooperative effects of crystal symmetry, electron occupancy, electron correlation, and intrinsic SOC [11]. This provides a new direction for the design of light element materials with strong effective SOC.

Very recently, based on spin group theory, altermagnetism is proposed as a new magnetic phase distinct from ferromagnetism and conventional collinear antiferromagnetism [12, 13]. Moreover, altermagnetic materials have a wide range of electronic properties, which cover metals, semi-metals, semiconductors, and insulators [13, 14]. Different from ferromagnetic materials with  $s$ -wave spin polarization, altermagnetic materials have  $k$ -dependent spin polarization, which results in many exotic physical effects [12, 13, 15–21]. With spin-orbit coupling, similar to the case of ferromagnetic materials, the time-reversal symmetry-breaking macroscopic phenomena can be also realized in altermagnetic materials [10, 22–24]. Nevertheless, altermagnetism is proposed based on spin group theory and the predicted altermagnetic materials basically are light element compounds [13, 14]. Therefore, it is very important to propose a mechanism to enhance SOC in light element compounds with altermagnetism and predict the corresponding compounds with strong SOC effect.

In this work, based on symmetry analysis and the first-principles electronic structure calculations, we predict that the light element compound  $\text{NiF}_3$  is an  $i$ -wave altermagnetic material with extremely strong SOC effect. Then, we propose a mechanism to enhance SOC effect in light element compounds with altermagnetism, which reveals the cooperative effects of crystal symmetry, electron occupation, electronegativity, electron correlation, and intrinsic SOC. We also explain the weak SOC effect in altermagnetic materials  $\text{VF}_3$ ,  $\text{CrF}_3$ ,  $\text{FeF}_3$ ,  $\text{CoF}_3$ .

*Results and discussion.* The  $\text{NiF}_3$  takes rhombohedral structure with nonsymmorphic  $R-3c$  (167) space group symmetry, as shown in Fig. 1(a) and (b). The corresponding elementary symmetry operations are  $C_{3z}$ ,  $C_{2t}^1$  and  $I$ , which yield the point group  $D_{3d}$ . The  $t$  represents  $(1/2, 1/2, 1/2)$  fractional translation. To confirm the magnetic ground state of  $\text{NiF}_3$ , we consider six different collinear magnetic structures, including one ferro-

\* guopengjie@ruc.edu.cn

† zlu@ruc.edu.cn

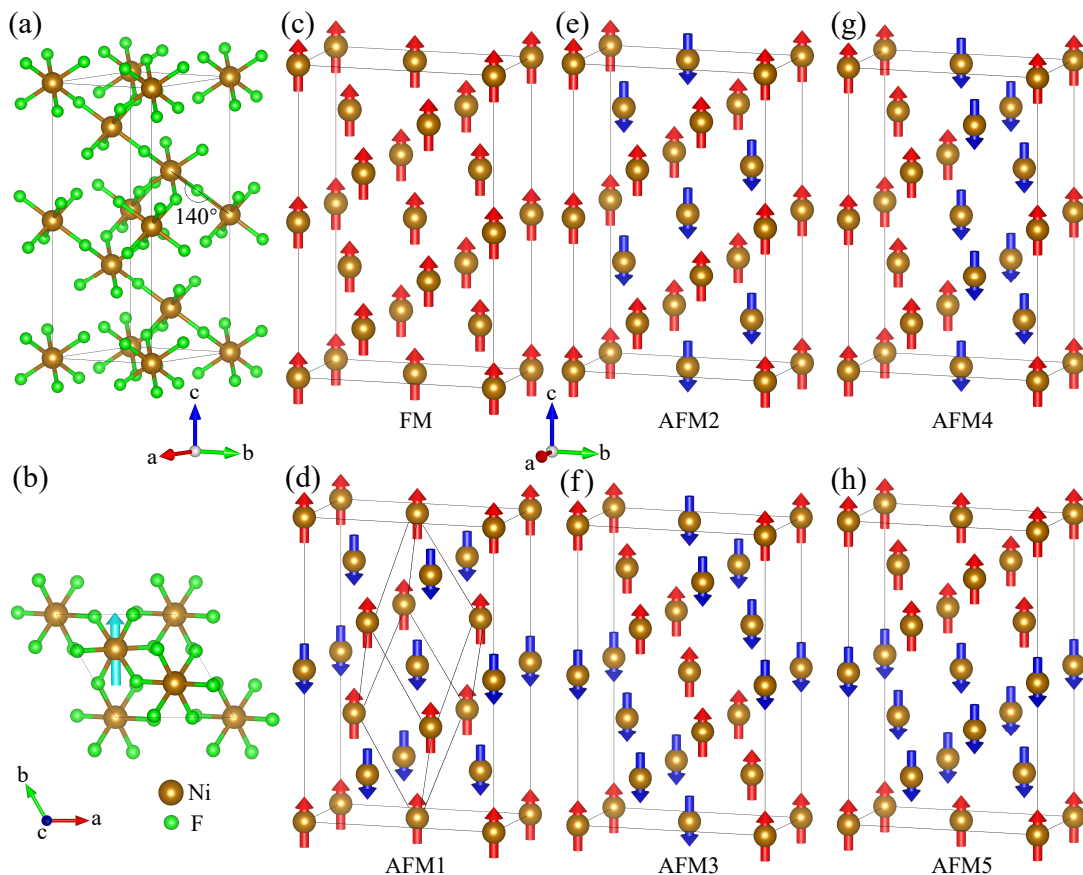


FIG. 1. The crystal structure and six collinear magnetic structures of  $\text{NiF}_3$ . (a) and (b) are side and top views of the crystal structure, respectively. The cyan arrow represents the direction of easy magnetization axis. (c)-(h) are six different collinear magnetic structures including one ferromagnetic and five different collinear antiferromagnetic structures. The bond angle of  $\text{Ni} - \text{F} - \text{Ni}$  for the nearest neighbour Ni ions is 140 degrees. The primitive cell of  $\text{NiF}_3$  is shown in (d). The red and blue arrows represent spin-up and spin-down magnetic moments, respectively.

magnetic and five collinear antiferromagnetic structures which are shown in Fig. 1(c)-(h). Then we calculate relative energies of six magnetic states with the variation of correlation interaction  $U$ . With the increase of correlation interaction  $U$ , the  $\text{NiF}_3$  changes from the ferromagnetic state to the collinear antiferromagnetic state AFM1 (Fig. 2(a)). The AFM1 is intralayer ferromagnetism and interlayer antiferromagnetism (Fig. 1(d)). In previous works, the correlation interaction  $U$  was selected as 6.7eV for Ni  $3d$  orbitals [25, 26]. Thus, the magnetic ground state of  $\text{NiF}_3$  is the AFM1 state, which is consistent with previous works[14]. On the other hand, since the bond angle of  $\text{Ni} - \text{F} - \text{Ni}$  for the nearest neighbour Ni ions is 140 degrees, the spins of the nearest neighbour and next nearest neighbour Ni ions are in antiparallel and parallel arrangement according to Goodenough-Kanamori rules [27], respectively. This will result in  $\text{NiF}_3$  being the collinear antiferromagnetic state AFM1. Thus, the results of theoretical analysis are in agreement with those of theoretical calculation.

Indeed, the structure of AFM1 is very simple and the corresponding magnetic primitive cell only contains two

magnetic atoms with opposite spin arrangement which is shown in Fig. 2(b). From Fig. 2(b), the two Ni atoms with opposite spin arrangement are surrounded by F-atom octahedrons with different orientations, respectively. Thus, the two opposite spin Ni sublattices cannot be connected by a fractional translation. Due to two Ni ions located at space-inversion invariant points, the two opposite spin Ni sublattices cannot be either connected by space-inversion symmetry. However, the two opposite spin Ni sublattices can be connected by  $C_2^1t$  symmetry. Thus, the  $\text{NiF}_3$  is an altermagnetic material. The BZ of altermagnetic  $\text{NiF}_3$  is shown in Fig. 2(c) and both the high-symmetry and non-high-symmetry lines and points are marked. In order to display the altermagnetic properties more intuitively, we calculate polarization charge density of altermagnetic  $\text{NiF}_3$ , which is shown in Fig. 2(d). From Fig. 2(d), the polarization charge densities of two Ni ions with opposite spin arrangement are anisotropic and their orientations are different, resulting from F-atom octahedrons with different orientations. The anisotropic polarization charge densities can result in  $\mathbf{k}$ -dependent spin polarization in reciprocal space. More-

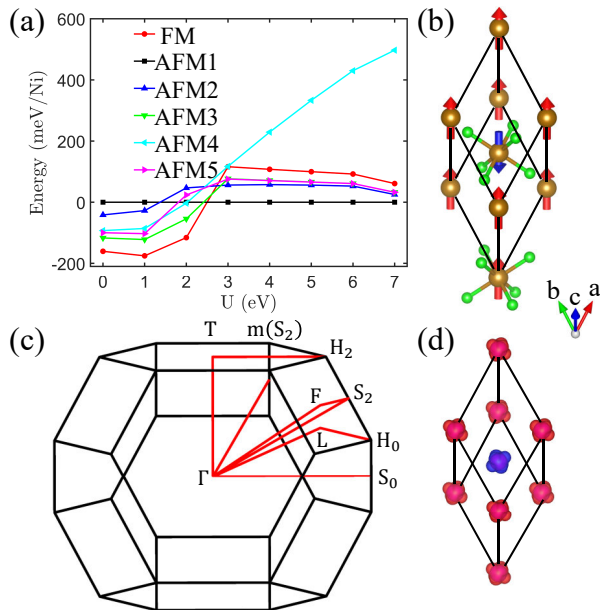


FIG. 2. The magnetic ground state of  $\text{NiF}_3$  and the corresponding properties. (a) Relative energies of six different magnetic states with the variation of correlation interaction  $U$ . (b) and (c) are the magnetic primitive cell of  $\text{NiF}_3$  and the corresponding Brillouin zone, respectively. The red and blue arrows represent spin-up and spin-down magnetic moments, respectively. The high-symmetry and non-high-symmetry lines and points are marked in the BZ. (d) The anisotropic polarization charge densities. The red and blue represent spin-up and spin-down polarization charge density, respectively.

over, according to different spin group symmetries, the  $\mathbf{k}$ -dependent spin polarization can form  $d$ -wave,  $g$ -wave, or  $i$ -wave magnetism [12].

Without SOC, the nontrivial elementary spin symmetry operations in altermagnetic  $\text{NiF}_3$  have  $\{E||C_{3z}\}$ ,  $\{C_2^\perp||M_1t\}$ ,  $\{E||I\}$ , and  $\{C_2^\perp T||T\}$ . The spin symmetries  $\{C_2^\perp||M_1t\}$ ,  $\{T||TM_1t\}$ , and  $\{E||C_{3z}\}$  make altermagnetic  $\text{NiF}_3$  being an  $i$ -wave magnetic material, as shown in Fig. 3(a). Moreover, the spins of bands are opposite along non-high-symmetry  $S_2 - \Gamma$  and  $\Gamma - m(S_2)$  directions, reflecting features of  $i$ -wave magnetism (Fig. 3(b)).

In order to well understand the electronic properties, we also calculate the electronic band structures of altermagnetic  $\text{NiF}_3$  along the high-symmetry directions. Ignoring SOC, the  $\text{NiF}_3$  is an altermagnetic metal. There are four bands crossing the Fermi level due to spin degeneracy on the high-symmetry directions (Fig. 3(c)). Especially, these four bands are degenerate on the  $\Gamma - T$  axis. In fact, any  $\mathbf{k}$  point on the  $\Gamma - T$  axis has nontrivial elementary spin symmetry operations  $\{E||C_{3z}\}$  and  $\{C_2^\perp||M_1t\}$ . And the spin symmetry  $\{E||C_{3z}\}$  has one one-dimensional irreducible real representation and two one-dimensional irreducible complex representations. Although the time-reversal symmetry is broken, altermag-

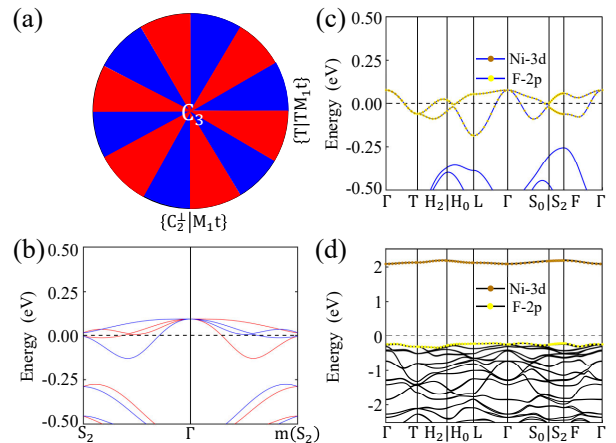


FIG. 3. Schematic diagram of the  $i$ -wave magnetism and electronic band structures of altermagnetic  $\text{NiF}_3$ . (a) Schematic diagram of the  $i$ -wave magnetism. The red and blue parts represent spin up and down, respectively. (b) The electronic band structure without SOC along the non-high-symmetry directions. The red and blue lines represent spin-up and spin-down bands, respectively. (c) and (d) are the electronic band structures without and with SOC along the high-symmetry directions.

netic materials have equivalent time-reversal spin symmetry  $\{C_2^\perp T||T\}$ . The spin symmetry  $\{C_2^\perp T||T\}$  will result in two one-dimensional irreducible complex representations to form a Kramers degeneracy. Meanwhile, the spin symmetry  $\{C_2^\perp||M_1t\}$  protects the spin degeneracy. Therefore, there is one four-dimensional and one two-dimensional irreducible representations on the  $\Gamma - T$  axis. The quadruple degenerate band crossing the Fermi level is thus protected by the spin group symmetry. Furthermore, the orbital weight analysis shows that these four bands are contributed by both the  $3d$  orbitals of Ni and the  $p$  orbitals of F (Fig. 3(c)). As is known to all, the F atom has the strongest electronegativity among all chemical elements, but the  $2p$  orbitals of F do not fully acquire the  $3d$ -orbital electrons of Ni, which is very interesting.

In our calculations, the number of valence electrons of  $\text{NiF}_3$  is 74, which makes the quadruple band only half-filled. This is the reason why the  $p$  orbitals of F do not fully acquire the  $d$ -orbital electrons of Ni. When SOC is included, the spin group symmetry breaks down to magnetic group symmetry. The reduction of symmetry will result in the quadruple band to split into multiple bands. Since the F atom has the strongest electronegativity, the  $2p$  orbitals of F will completely acquire the  $3d$ -orbital electrons of Ni. This will result in altermagnetic  $\text{NiF}_3$  to transform from metal phase to insulator phase. In order to prove our theoretical analysis, we calculate the electronic band structure of altermagnetic  $\text{NiF}_3$  with SOC. The calculation of the easy magnetization axis and symmetry analysis based on magnetic point group are shown in Supplementary Material[28]. Just like our theoretical analysis, the  $2p$  orbitals of F indeed fully acquire the

**3d**-orbital electrons of Ni and altermagnetic NiF<sub>3</sub> transforms into an insulator with a bandgap of 2.31eV (Fig. 3(d)). In general, the SOC strength of Ni is in the order of 10meV, so the SOC strength of altermagnetic NiF<sub>3</sub> is two orders of magnitude higher than that of Ni. Thus, the SOC effect of altermagnetic NiF<sub>3</sub> is extremely strong.

On the other hand, we also examine the effect of correlation interaction in altermagnetic NiF<sub>3</sub>. We calculate the electronic band structures of altermagnetic NiF<sub>3</sub> along the high-symmetry directions without SOC under correlation interaction  $U = 3, 5, 7\text{eV}$ , which are shown in Fig. 4(a), (b), and (c), respectively. From Fig. 4(a), (b) and (c), the correlation interaction has a slight effect on the band structure around the Fermi level without SOC, due to the constraints of spin symmetry and electron occupancy being 74. When including SOC, altermagnetic NiF<sub>3</sub> transforms from a metal phase to an insulator phase under different correlation interaction  $U$ . Moreover, the bandgap of altermagnetic NiF<sub>3</sub> increases linearly with the correlation interaction  $U$ . Thus, the correlation interaction can substantially enhance the bandgap opened by the SOC of altermagnetic materials.

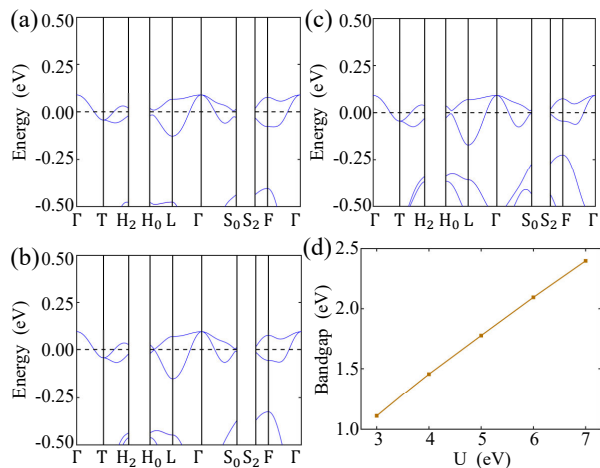


FIG. 4. The electronic properties of altermagnetic NiF<sub>3</sub> under different correlation interaction  $U$ . (a), (b) and (c) are the electronic band structures along the high-symmetry directions without SOC under correlation interaction  $U = 3, 5, 7\text{eV}$ , respectively. (d) The bandgap as a function of correlation interaction  $U$  under SOC.

Now we well understand the reason for the extremely strong SOC effect in altermagnetic NiF<sub>3</sub>. A natural question is whether such a strong SOC effect can be realized in other altermagnetic materials. According to the above analysis, we propose four conditions for realizing such an effective strong SOC in light element altermagnetic materials: First, the spin group of altermagnetic material has high-dimensional (greater than four dimensions) irreducible representation (crystal symmetry groups are presented in the Supplementary Material[28]); Second, the band with high-dimensional representation crossing the Fermi level is half-filled by valence electrons; Third, non-metallic elements have strong electronegativity; Fourth,

the altermagnetic material has strong electron correlation. To verify these four conditions, we also calculate the electronic band structures of four *i*-wave altermagnetic materials (VF<sub>3</sub>, CrF<sub>3</sub>, FeF<sub>3</sub> and CoF<sub>3</sub>), which have the same crystal structure and spin group symmetry as NiF<sub>3</sub>[14]. The calculations show that none of the four altermagnetic materials meets the second condition, and the SOC effect is very weak (Detailed calculations and analysis are presented in the Supplementary Material[28]). On the other hand, since high-dimensional irreducible representations can be protected by spin space group in two-dimensional altermagnetic systems, the proposed mechanism is also applicable to two-dimensional light element altermagnetic materials, which may be advantage for realizing quantum anomalous Hall effect at high temperatures [10].

The mechanism for enhancing the SOC effect that we propose in altermagnetic materials is different from that in ferromagnetic materials [11]. First, the high-dimensional representation of the symmetry group is 2 or 3 dimensions in ferromagnetism, while in altermagnetism the high-dimension representation is 4 or 6 dimensions, so their symmetry requirements are entirely different. Second, the band with high-dimensional representation in ferromagnetism comes from *d* orbitals, while the band with high-dimensional representation in altermagnetism can come from the combination of *p* orbitals and *d* orbitals. Third, the enhancement of SOC effect derives from correlation interaction for ferromagnetic materials, but from both correlation interaction and electronegativity of nonmetallic element for altermagnetic materials. Due to one more degree of freedom to enhance the SOC effect, a stronger SOC effect can be achieved in the altermagnetic materials. Moreover, if electronegativity of nonmetallic element is weak, different topological phases may be realized in altermagnetic materials when including SOC. On the other hand, the mechanism for enhancing SOC effect in altermagnetic materials can be also generalized to conventional antiferromagnetic materials. Due to the equivalent time-reversal symmetry, more spin groups with conventional antiferromagnetism have high-dimensional irreducible representations. Moreover, conventional antiferromagnetic materials are more abundant than altermagnetic materials, thus conventional antiferromagnetic materials of light elements with strong SOC effect remain to be discovered.

*Summary.* Based on spin symmetry analysis and the first-principles electronic structure calculations, we demonstrate that extremely strong SOC effect can be realized in altermagnetic material NiF<sub>3</sub>. Then, we propose a mechanism to enhance SOC effect in altermagnetic materials. This mechanism reveals the cooperative effect of crystal symmetry, electron occupation, electronegativity, electron correlation, and intrinsic spin-orbit coupling. The mechanism can explain not only the extremely strong SOC effect in altermagnetic NiF<sub>3</sub>, but also the weak SOC in altermagnetic VF<sub>3</sub>, CrF<sub>3</sub>, FeF<sub>3</sub>, CoF<sub>3</sub>. Moreover, the mechanism for enhancing SOC effect can

be also generalized to two-dimensional altermagnetic materials.

## ACKNOWLEDGMENTS

This work was financially supported by the National Key R&D Program of China (Grant No. 2019YFA0308603), the National Natural Science Foundation of China (Grant No.11934020, No.12204533, No.62206299 and No.12174443) and the Beijing Natural Science Foundation (Grant No.Z200005). Computational resources have been provided by the Physical Laboratory of High Performance Computing at Renmin University of China.

- 
- [1] M. Z. Hasan and C. L. Kane, Colloquium: Topological insulators, *Rev. Mod. Phys.* **82**, 3045 (2010).
- [2] X.-L. Qi and S.-C. Zhang, Topological insulators and superconductors, *Rev. Mod. Phys.* **83**, 1057 (2011).
- [3] A. Bansil, H. Lin, and T. Das, Colloquium: Topological band theory, *Rev. Mod. Phys.* **88**, 021004 (2016).
- [4] N. Nagaosa, J. Sinova, S. Onoda, A. H. MacDonald, and N. P. Ong, Anomalous hall effect, *Rev. Mod. Phys.* **82**, 1539 (2010).
- [5] J. Sinova, S. O. Valenzuela, J. Wunderlich, C. H. Back, and T. Jungwirth, Spin hall effects, *Rev. Mod. Phys.* **87**, 1213 (2015).
- [6] J. E. Hirsch, Spin hall effect, *Phys. Rev. Lett.* **83**, 1834 (1999).
- [7] M. Cinal, D. M. Edwards, and J. Mathon, Magnetocrystalline anisotropy in ferromagnetic films, *Phys. Rev. B* **50**, 3754 (1994).
- [8] F. D. M. Haldane, Model for a quantum hall effect without landau levels: Condensed-matter realization of the "parity anomaly", *Phys. Rev. Lett.* **61**, 2015 (1988).
- [9] C.-Z. Chang, C.-X. Liu, and A. H. MacDonald, Colloquium: Quantum anomalous hall effect, *Rev. Mod. Phys.* **95**, 011002 (2023).
- [10] P.-J. Guo, Z.-X. Liu, and Z.-Y. Lu, Quantum anomalous hall effect in collinear antiferromagnetism, *npj Comput. Mater.* **9**, 70 (2023).
- [11] J. Li, Q. Yao, L. Wu, Z. Hu, B. Gao, X. Wan, and Q. Liu, Designing light-element materials with large effective spin-orbit coupling, *Nat. Commun.* **13**, 919 (2022).
- [12] L. Šmejkal, J. Sinova, and T. Jungwirth, Beyond conventional ferromagnetism and antiferromagnetism: A phase with nonrelativistic spin and crystal rotation symmetry, *Phys. Rev. X* **12**, 031042 (2022).
- [13] L. Šmejkal, J. Sinova, and T. Jungwirth, Emerging research landscape of altermagnetism, *Phys. Rev. X* **12**, 040501 (2022).
- [14] Z.-F. Gao, S. Qu, B. Zeng, Y. Liu, J.-R. Wen, H. Sun, P.-J. Guo, and Z.-Y. Lu, Ai-accelerated discovery of altermagnetic materials (2023), arXiv:2311.04418 [cond-mat.mtrl-sci].
- [15] H.-Y. Ma, M. Hu, N. Li, J. Liu, W. Yao, J.-F. Jia, and J. Liu, Multifunctional antiferromagnetic materials with giant piezomagnetism and noncollinear spin current, *Nat. Commun.* **12**, 2846 (2021).
- [16] L. Šmejkal, A. B. Hellenes, R. González-Hernández, J. Sinova, and T. Jungwirth, Giant and tunneling magnetoresistance in unconventional collinear antiferromagnets with nonrelativistic spin-momentum coupling, *Phys. Rev. X* **12**, 011028 (2022).
- [17] R. González-Hernández, L. Šmejkal, K. Výborný, Y. Yahagi, J. Sinova, T. c. v. Jungwirth, and J. Železný, Efficient electrical spin splitter based on nonrelativistic collinear antiferromagnetism, *Phys. Rev. Lett.* **126**, 127701 (2021).
- [18] H. Bai, L. Han, X. Y. Feng, Y. J. Zhou, R. X. Su, Q. Wang, L. Y. Liao, W. X. Zhu, X. Z. Chen, F. Pan, X. L. Fan, and C. Song, Observation of spin splitting torque in a collinear antiferromagnet RuO<sub>2</sub>, *Phys. Rev. Lett.* **128**, 197202 (2022).
- [19] S. Karube, T. Tanaka, D. Sugawara, N. Kadoguchi, M. Kohda, and J. Nitta, Observation of spin-splitter torque in collinear antiferromagnetic RuO<sub>2</sub>, *Phys. Rev. Lett.* **129**, 137201 (2022).
- [20] D. Zhu, Z.-Y. Zhuang, Z. Wu, and Z. Yan, Topological superconductivity in two-dimensional altermagnetic metals, *Phys. Rev. B* **108**, 184505 (2023).
- [21] P.-J. Guo, Y. Gu, Z.-F. Gao, and Z.-Y. Lu, Altermagnetic ferroelectric LiFe<sub>2</sub>F<sub>6</sub> and spin-triplet excitonic insulator phase (2023), arXiv:2312.13911 [cond-mat.mtrl-sci].
- [22] L. Šmejkal, R. Gonzalez-Hernandez, T. Jungwirth, and J. Sinova, Crystal time-reversal symmetry breaking and spontaneous hall effect in collinear antiferromagnets, *Sci. Adv.* **6**, eaaz8809 (2020).
- [23] X. Zhou, W. Feng, X. Yang, G.-Y. Guo, and Y. Yao, Crystal chirality magneto-optical effects in collinear antiferromagnets, *Phys. Rev. B* **104**, 024401 (2021).
- [24] X.-Y. Hou, H.-C. Yang, Z.-X. Liu, P.-J. Guo, and Z.-Y. Lu, Large intrinsic anomalous hall effect in both Nb<sub>2</sub>FeB<sub>2</sub> and Ta<sub>2</sub>FeB<sub>2</sub> with collinear antiferromagnetism, *Phys. Rev. B* **107**, L161109 (2023).
- [25] B. Žemva, K. Lutar, L. Chacon, M. Fele-Beuermann, J. A. Allman, C. J. Shen, and N. Bartlett, Thermodynamically unstable fluorides of nickel: NiF<sub>4</sub> and NiF<sub>3</sub> syntheses and some properties, *J. Am. Chem. Soc.* **117**, 10025 (1995).
- [26] S. Mattsson and B. Paulus, Density functional theory calculations of structural, electronic, and magnetic properties of the 3d metal trifluorides MF<sub>3</sub> (M = Ti-Ni) in the solid state, *J. Comput. Chem.* **40**, 1190 (2019).
- [27] J. B. Goodenough, Goodenough-Kanamori rule, *Scholarpedia* **3**, 7382 (2008).
- [28] Supplemental material, .